

Chaos, entanglement, and Husimi Q function in quantum Rabi model

Shangyun Wang¹, Songbai Chen^{2,3}, and Jiliang Jing^{2,3*}

¹College of Physics and Electronic Engineering, Hengyang Normal University, Hengyang 421002, China

²Key Laboratory of Low-Dimensional Quantum Structures and Quantum Control of Ministry of Education, Key Laboratory for Matter Microstructure and Function of Hunan Province, Department of Physics and Synergetic Innovation Center for Quantum Effects and Applications, Hunan Normal University, Changsha 410081, China

³Center for Gravitation and Cosmology, College of Physical Science and Technology, Yangzhou University, Yangzhou 225009, People's Republic of China

As one of the famous effects in quantum Rabi model(QRM), Rabi oscillation may lead to the occurrence of quantum dynamics behaviors without classical dynamic counterparts, such as quantum collapse and revival effects. In this paper, we focus on studying whether the entanglement entropy and Husimi Q function, as diagnostic tools for quantum chaos in quantum systems, are invalidated by quantum collapse and revival. It is shown that the saturation values of entanglement entropy for initial states located in the chaotic sea of QRM are higher than that in the regular regions. When the system reaches dynamic equilibrium, the Husimi Q function which initial states located in the chaotic sea are more dispersed than that in the regular regions. Moreover, we observe a good correspondence between the the time-average entanglement entropy and classical phase space structures. Our results imply that entanglement entropy and Husimi Q function maintain the function for diagnosing chaos in the QRM and the corresponding principle does not invalidated by quantum collapse and revival effects in this system.

I. INTRODUCTION

Correspondence principle is an indispensable cornerstone of quantum mechanics, which bridges classical and quantum world. In classical physics, the hallmark of chaotic dynamics is the extreme sensitivity of the time evolution of a system to initial conditions. However, quantum mechanics does not support a similar definition due to the uncertainty principle and the overlap between quantum states. This fundamental incompatibility poses a challenge to the correspondence principle and has motivated a long-standing search for chaotic signatures in quantum systems [1–5].

Defining quantum chaos by analogy with classical chaos faces numerous obstacles. Finding quantum tools which exhibit significant differences between chaotic and regular regions in semiclassical systems has become one of the mainstream solutions for studying quantum chaos. The study of entanglement entropy indicates that in semiclassical quantum systems, the entanglement entropy in the chaotic regions are significantly greater than that in the regular regions [6–14]. Specifically, the corresponding relationship between the time-averaged entanglement entropy and the classical phase space is one of the important evidences to test the correspondence principle [15, 16]. Because chaos is inherently a dynamical phenomenon, as one of the quasi-probability distribution functions used to visualize quantum wave packets dynamics, the Husimi Q function exhibits significant time-evolution differences between chaotic and regular regions [15–22]. Moreover, the level spacing distribution [23–28], Loschmidt Echo [29–32] and OTOC [35–47] have been proven to be effective tools for exploring chaos in quantum systems.

For the systems of light interacting with atoms, the researches related to quantum chaos mainly focus on the Dicke

model [48–56]. The Rabi model [57], as the simplest version of the Dicke model, describes a single mode cavity field and a two-level atom which interact via dipolar coupling [58, 59]. Since the Rabi model exhibits similar interaction mechanism to Dicke model, the chaotic dynamic behaviors should appear in this system. However, the study of chaos in this model has been neglected for a long time owing in part to the number of atom, and in part to the Rabi oscillations, which generate some effects without classical dynamic counterparts such as quantum collapse and revival [60].

The quantum chaos of a system with quantum collapse and revival effect is of great interest, not only from the horizon of quantum dynamics, but from the viewpoint of the correspondence between quantum and classical mechanics as well. Recently, Irish and Armour [61] studied the semiclassical limit in the QRM and their result provide a important and feasible framework to study the classical-quantum correspondence in this system. Kirkova *et al.* [62] found that the out-of-time-ordered correlator (OTOC) quickly saturates in the normal phase and undergoes exponential growth in the superradiant phase of QRM when the ratio of level-splitting ω to bosonic frequency ω_0 grows to infinity $\eta = \omega/\omega_0 \rightarrow \infty$. This indicates that chaotic signatures appear in the QRM at effective thermodynamic limits $\eta \rightarrow \infty$. On the other hand, using the mean field approximation theory, Ref. [63] shows that quantum collapse and revival effects can interfere with the exponential behavior of OTOC in the anisotropic quantum Rabi model. However, it is not yet uncertain that when the Rabi system evolves to dynamic equilibrium, whether the quantum collapse and revival effects affect the entanglement entropy and Husimi Q function as tools for diagnosing quantum chaos. Moreover, due to the quantum collapse and revival effects, the Husimi quasiprobability distribution function exhibits nonclassical dynamic behaviors such as splitting and merging. Then, the natural question is whether these non-classical phenomenon cause the classical-quantum correspondence breakdown in the semiclassical Rabi model. The intrinsic

* E-mail address: sywang@hynu.edu.cn

sic physics is still unclear and needs to be investigated further.

In this paper, we will focus on studying the quantum signatures of chaos in quantum Rabi model which consists of a single cavity field mode interact with a two-level atom via dipolar coupling. We find that the saturation values of entanglement entropy for initial states located in chaotic regions are higher than that in regular regions, and the long-time average entanglement entropy correspond well with the classical phase space structures. Meanwhile, when the QRM evolves to dynamic equilibrium, the Husimi Q function exhibits significant differences between the chaotic and regular regions while it exhibits splitting and merging behaviors during the evolutionary process.

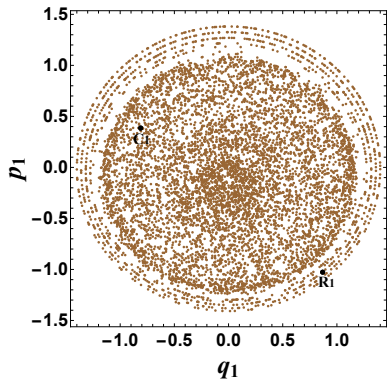


FIG. 1. The Poincaré section for the quantum Rabi model in the case: $q_2 = 0, p_2 > 0$, with $\omega = 18, \omega_0 = 1, g = 4$ and the system energy $E = 14$. Point $R_1(q_1 = 0.86853, p_1 = -1.02681, q_2 = 0, p_2 = 3.66657)$ and $C_1(q_1 = -0.2, p_1 = 0, q_2 = 0, p_2 = 6.72904)$ are situated in stable island and chaotic sea respectively.

This paper is organized as follows: In Sec. II, we introduce briefly the QRM and its semiclassical phase space. In Sec. III, we investigate the truncated photon number in the QRM when the ratio of level-splitting ω to bosonic frequency ω_0 grows to $\eta = \omega/\omega_0 \rightarrow 18$. In Sec. IV, we analyze the evolutionary differences of Husimi Q function with splitting and merging behaviors between chaotic and regular regions in this model. In Sec. V, we study the correspondence between the distribution of time-averaged entanglement entropy and the classical Poincaré section. Finally, we present results and a brief summary.

II. QUANTUM RABI MODEL

Let us now briefly introduce the quantum Rabi model which is one of the simplest and most fundamental models describing quantum light-matter interaction. The Rabi Hamiltonian can be expressed as ($\hbar = 1$)

$$\hat{H} = \frac{\omega}{2}\sigma_z + \omega_0 a^\dagger a + g(a^\dagger + a)(\sigma_+ + \sigma_-), \quad (1)$$

where ω is the level-splitting of a two-level atom and a^\dagger, a are respectively the creation and annihilation operators of the single-mode cavity with frequency ω_0 . The coupling g is the

strength of the dipolar atom-field interaction and σ_+, σ_- are atomic raising and lowering operators, respectively.

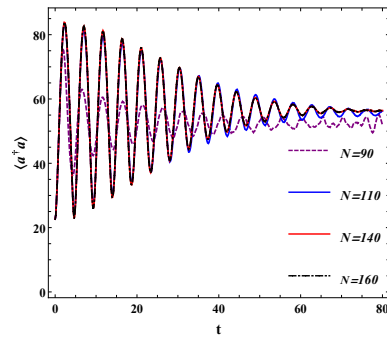


FIG. 2. Time evolution of the average photon number $\langle a^\dagger a \rangle$ with different the initial system photon number N for the initial coherent states centered at regular point C_1 .

To study the quantum signatures of chaos in the quantum Rabi model. As in Refs. [6], we take the initial states to be coherent states since the its uncertainty in phase space are the smallest. The initial quantum states are chosen as

$$|\psi(0)\rangle = |\tau\rangle \otimes |\beta\rangle, \quad (2)$$

with

$$|\tau\rangle = (1 + \tau\tau^*)^{-\frac{1}{2}} e^{\tau\sigma_+} |\frac{1}{2}, -\frac{1}{2}\rangle, \quad (3)$$

$$|\beta\rangle = e^{-\beta\beta^*/2} e^{\beta a^\dagger} |0\rangle, \quad (4)$$

and

$$\tau = \frac{q_1 + ip_1}{\sqrt{2 - q_1^2 - p_1^2}}, \quad \beta = (q_2 + ip_2)/\sqrt{2}, \quad (5)$$

where $|\tau\rangle$ and $|\beta\rangle$ are Bloch coherent states of atom and Glauber coherent states of bosons, and the states $|\frac{1}{2}, -\frac{1}{2}\rangle$ and $|0\rangle$ are the ground state of two-level atom and the vacuum state of single-mode cavity field, respectively. With the mean field approximation procedure, the semiclassical Rabi Hamiltonian reads

$$H_{cl} = \frac{\omega}{2}(q_1^2 + p_1^2 - 1) + \frac{\omega_0}{2}(q_2^2 + p_2^2) + gq_1q_2\sqrt{4 - 2(q_1^2 + p_1^2)}, \quad (6)$$

where $q_2 = (a^\dagger + a)/\sqrt{2}$ and $p_2 = i(a^\dagger - a)/\sqrt{2}$. With the classical Hamiltonian 6, we obtain the poicaré section of the QRM, as shown in Fig. 1. This mixed phase space section contains both stable island and chaotic sea composed of many discrete points. Motion across the boundaries between regular and chaotic regions is classically forbidden.

III. TRUNCATED PHOTON NUMBER

QRM is intuitively far from the so-called thermodynamic limit ($N \rightarrow \infty$) because there is only one atom, and it seems

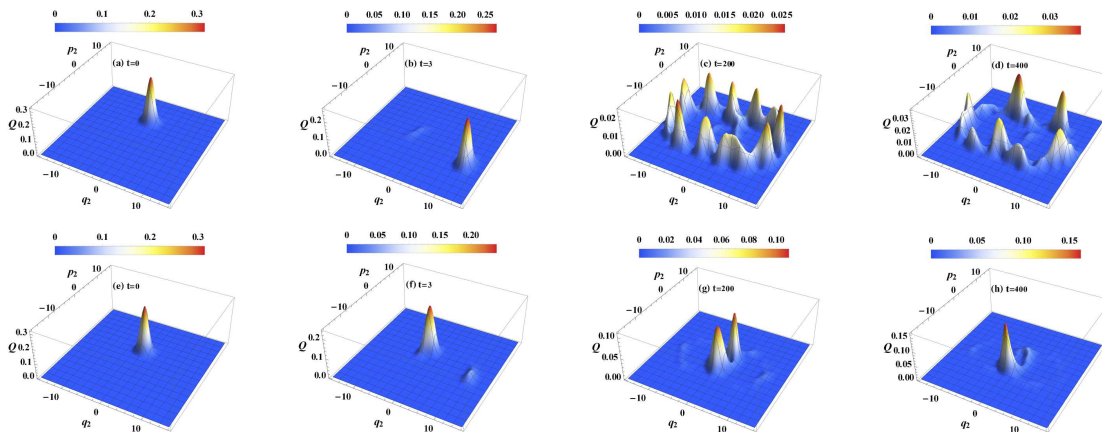


FIG. 3. The time evolution of the Husimi Q function. The top and bottom panels denote respectively the case in which the initial coherent state centered at the points C_1 and R_1 in Fig. 1. Here, the system photon number is truncated at 150.

impossible to achieve the classical-quantum correspondence in this system. On the other hand, the exponential growth of OTOC in the superradiant phase of QRM when the ratio of level-splitting ω to bosonic frequency grows to infinity [62]. This means this model can be considered as a many-body quantum system. A reasonable explanation is that the number of photons in the QRM also tends to infinity as ω/ω_0 tends to infinity, and then classical-quantum correspondence can be achieved and quantum chaotic signatures can be distinguished. In this section, we numerically calculate the truncated photon number in QRM when the ratio of level-splitting ω to bosonic frequency ω_0 grows to $\eta = \omega/\omega_0 \rightarrow 18$. In Fig. 2, we exhibit the time evolution behavior of the average photon number $\langle a^\dagger a \rangle$ with different system photon number N for the initial wave packet centered at point C_1 . It is shown that the dynamical evolution of $\langle a^\dagger a \rangle$ changes with the increase of the initial system photon number N . However, when N exceeds the critical value N_c ($N_c \approx 140$), the evolutionary behaviors of $\langle a^\dagger a \rangle$ are consistent. In other words, when the initial system photon number exceeds the critical value, i.e., $N > N_c$, the dynamic effects in the QRM no longer changes with the increase of photon number. This indicates that the system photon number can be truncated at a value which greater than the critical value when the ratio of level-splitting ω to bosonic frequency ω_0 grows to 18. Therefore, the QRM can be considered as a semiclassical many-body quantum system when ω/ω_0 grows to large values, and then quantum chaos and classical-quantum correspondence can be studied in this system.

IV. HUSIMI Q FUNCTION

In the quantum domain, the quantum state is equivalent to its quasi-probability function in the phase space [64]. Among the quasi-probability functions, the Husimi Q function allows one to visualize the dynamical evolution of quantum states in phase space. On the other hand, the collapse and revival of Husimi Q function have been interpreted theoretically [65–68] and observed experimentally [69–72] in atom-field interaction systems. In this section, we focus on analyzing the time evolution difference of Husimi Q functions between chaotic

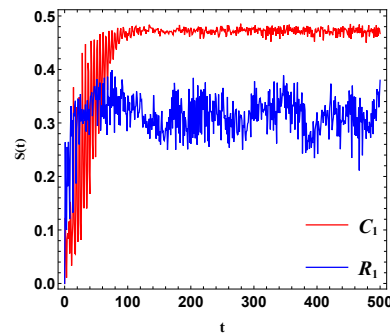


FIG. 4. The time evolution of linear entanglement entropy $S(t)$ for initial states centered at chaotic point C_1 and periodic point R_1 in Fig. 1. Here, the system photon number is truncated at 150.

and regular regions in the QRM. For a photon coherent state, the Husimi Q function is defined as

$$Q(q_2, p_2) = \frac{1}{\pi} \langle q_2, p_2 | \rho_2 | q_2, p_2 \rangle, \quad (7)$$

where $|q_2, p_2\rangle$ is a photon coherent state and ρ_2 is the reduced density matrix of the second subsystem. In Fig. 3, we present the time evolution of Husimi Q function in phase space. Quantum collapse and revival do indeed cause the Husimi Q function generate some effects which without classical dynamical counterparts such as splitting and merging, as shown in Fig. 3(b) and Fig. 3(f). The difference between Fig. 3(b) and Fig. 3(f) is extremely microscopic and cannot distinguish chaotic and regular orbits. However, when the Rabi system reaches dynamic equilibrium, the Husimi Q function with initial states located in chaotic sea are distributed in the outer part of the phase space, as shown in Fig. 3(c)-Fig. 3(d). This is different from that in the Dicke model, where the Husimi function in the chaotic region rapidly distributes throughout the whole phase space [16]. For initial states located in the regular regions, the Husimi Q function are concentrated in the vicinity of origin point, as shown in Fig. 3(g)-Fig. 3(h). Obviously, the Husimi Q functions between chaotic and regular regions exhibit significant differences in long-time. This effectively indicates that the Husimi Q function can be considered as an

effective tool for diagnosing chaos in QRM while quantum collapse-revival effects exist in this system.

V. LINEAR ENTANGLEMENT ENTROPY

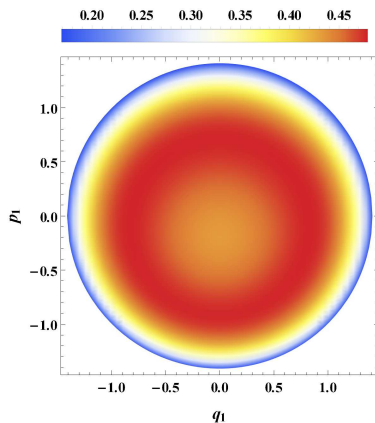


FIG. 5. The distribution of time-average entanglement entropy S_m of Poincaré section in Fig. 1. Here, the system photon number is truncated at 150 and the integral interval is $t \in [0, 500]$.

In this section, we will investigate the quantum signatures of chaos in the QRM via linear entanglement entropy, which is an effective tool to explore chaos in quantum systems including the Dicke model [6, 8, 16] and the kicked top model [15]. The linear entanglement entropy is defined as

$$S(t) = 1 - \text{Tr}_1 \rho_1(t)^2. \quad (8)$$

with the reduced-density matrix

$$\rho_1 = \text{Tr}_2 |\psi(t)\rangle\langle\psi(t)|. \quad (9)$$

where Tr_i is a trace over the i th subsystem ($i = 1, 2$) and the wave function $|\psi(t)\rangle$ is the quantum state of the full system. The quantity $S(t)$ describes the degree of purity of the subsystems and the degree of decoherence. In Fig. 4, we exhibit the time evolution of linear entanglement entropy for different initial states. It is shown that the difference of linear

entanglement entropy between chaotic and regular regions is very diminutive in short time. However, the saturation value of linear entanglement entropy for initial state located in the chaotic sea is significantly higher than that in the regular region. Moreover, to avoid the randomness of initial state selection, we demonstrate the distribution of the time-average entanglement entropy $S_m = \frac{1}{T} \int_{t_1}^{t_2} S(t) dt$ on the Poincaré section in Fig. 5. It is clearly observe a significant dip in S_m and more entanglement generation for initial states localized in chaotic sea compared to those in the regular regions. This difference of linear entanglement entropy between chaos and regular regions can be measured experimentally [15]. The correspondence between the phase space and the distribution of time-average linear entanglement entropy not only indicates that entanglement entropy can explore quantum chaos in the semiclassical QRM, but also indicates the classical-quantum correspondence can be achieved in QRM.

VI. SUMMARY

We have studied linear entanglement entropy and Husimi Q function in the QRM. It is shown that both the entanglement entropy and the Husimi Q function can still be used as tools to diagnose quantum chaos in the QRM while quantum collapse-revival effects exist in this system. When the Rabi system reaches dynamic equilibrium, the Husimi Q function for initial states located in the chaotic sea are distributed along the periphery of phase space, and for initial states located in the regular regions, the Husimi Q function are concentrated in the vicinity of origin. Moreover, we find good correspondence between the time-average linear entanglement entropy and classical phase space structures, and the saturation values of linear entanglement entropy in chaotic regions are larger than that in regular regions. Quantum collapse and revival indeed generate some quantum effects which without classical dynamics counterparts, such as the splitting and merging of wave packets, but it does not render the corresponding principle ineffective in the semiclassical Rabi model.

VII. ACKNOWLEDGMENTS

This work was supported by the National Natural Science Foundation of China under Grant No.12275078, 11875026, 12035005, 2020YFC2201400, and the innovative research group of Hunan Province under Grant No. 2024JJ1006.

[1] M. C. Gutzwiller, *Chaos in Classical and Quantum Mechanics* (Springer, New York, 1990).
 [2] G. Casati and B. Chirikov, *Quantum Chaos: Between Order and Disorder* (Cambridge University Press, Cambridge, UK, 1995).
 [3] H. Stockmann, *Quantum Chaos: An Introduction* (Cambridge University Press, Cambridge, UK, 1999).
 [4] F. Haake, *Quantum Signatures of Chaos* (Springer, Berlin, 2001).
 [5] H.-J. Stöckmann, *Quantum Chaos: An Introduction* (Cambridge University Press, Cambridge, England, 2006).

[6] K. Furuya, M. C. Nemes, and G. Q. Pellegrino, Quantum Dynamical Manifestation of Chaotic Behavior in the Process of Entanglement, *Phys. Rev. Lett.* **80**, 5534 (1998).
 [7] X. Wang, S. Ghose, B. C. Sanders, and B. Hu, Entanglement as a signature of quantum chaos, *Phys. Rev. E* **70**, 016217 (2004).
 [8] X. W. Hou and B. Hu, Decoherence, entanglement, and chaos in the Dicke model, *Phys. Rev. A* **69**, 042110 (2004).
 [9] M. A. Valdez, G. Shchedrin, M. Heimsoth, C. E. Creffield, F. Sols, and L. D. Carr, Many-Body Quantum Chaos and Entanglement in a Quantum Ratchet, *Phys. Rev. Lett.* **120**, 234101 (2018).

- [10] M. Kumari and S. Ghose, Untangling entanglement and chaos, *Phys. Rev. A* **99**, 042311 (2019).
- [11] A. Lerose and S. Pappalardi, Bridging entanglement dynamics and chaos in semiclassical systems, *Phys. Rev. A* **102**, 032404 (2020).
- [12] Amichay Vardi, Chaos and bipartite entanglement between Bose-Josephson junctions, *Phys. Rev. E* **106**, 064210 (2022)
- [13] C. Liang, Y. Zhang, and S. Chen, Statistical and dynamical aspects of quantum chaos in a kicked Bose-Hubbard dimer, *Phys. Rev. A* **109**, 033316 (2024).
- [14] N. Dowling, and K. Modi, Operational Metric for Quantum Chaos and the Corresponding Spatiotemporal-Entanglement Structure, *PRX Quantum* **5**, 010314 (2024).
- [15] S. Chaudhury, A. Smith, B. E. Anderson, S. Ghose and P. S. Jessen, Quantum signatures of chaos in a kicked top, *Nature (London)* **461**, 768 (2009).
- [16] S. Wang, S. Chen, and J. Jing, Effect of system energy on quantum signatures of chaos in the two-photon Dicke model, *Phys. Rev. E* **100**, 022207 (2019).
- [17] K. Takahashi and N. Saito, Chaos and Husimi Distribution Function in Quantum Mechanics, *Phys. Rev. Lett.* **55**, 645 (1985)
- [18] A. Piga, M. Lewenstein, and J. Q. Quach, Quantum chaos and entanglement in ergodic and nonergodic systems, *Phys. Rev. E* **99**, 032213 (2019).
- [19] S. Pilatowsky-Cameo *et al.*, Quantum scarring in a spin-boson system: fundamental families of periodic orbits, *New J. Phys.* **23** 033045 (2021).
- [20] Q. Wang, and M. Robnik, Statistics of phase space localization measures and quantum chaos in the kicked top model, *Phys. Rev. E* **107**, 054213 (2023).
- [21] Q. Wang, and M. Robnik, Mixed eigenstates in the Dicke model: Statistics and power-law decay of the relative proportion in the semiclassical limit, *Phys. Rev. E* **109**, 024225 (2024).
- [22] V. Mourik *et al.*, Exploring quantum chaos with a single nuclear spin, *Phys. Rev. E* **98**, 042206 (2018).
- [23] C. Emary and T. Brandes, Quantum Chaos Triggered by Precursors of a Quantum Phase Transition: The Dicke Model, *Phys. Rev. Lett.* **90**, 044101 (2003).
- [24] C. Emary and T. Brandes, Chaos and the quantum phase transition in the Dicke model, *Phys. Rev. E* **67**, 066203 (2003).
- [25] L. D'Alessio, Y. Kafri, A. Polkovnikov, and M. Rigol, From quantum chaos and eigenstate thermalization to statistical mechanics and thermodynamics, *Adv. Phys.* **65**, 239 (2016),
- [26] N. Anand, G. Styliaris, Meenu Kumari, and Paolo Zanardi, Quantum coherence as a signature of chaos, *Phys. Rev. Research* **3**, 023214 (2021).
- [27] Q. Wang, Quantum Chaos in the Extended Dicke Model, *Entropy* **24**, 1415 (2022).
- [28] L. Benet, F. Borgonovi, F. M. Izrailev, and L. F. Santos, Quantum-classical correspondence of strongly chaotic many-body spin models, *Phys. Rev. B* **107**, 155143 (2023).
- [29] R. A. Jalabert and H. M. Pastawski, Environment-Independent Decoherence Rate in Classically Chaotic Systems, *Phys. Rev. Lett.* **86**, 2490(2001).
- [30] Z. P. Karkuszewski, C. Jarzynski, and W. H. Zurek, Quantum Chaotic Environments, the Butterfly Effect, and Decoherence, *Phys. Rev. Lett.* **89**, 170405 (2002).
- [31] T. Gorin, T. Prosen *et al.*, Dynamics of Loschmidt echoes and fidelity decay, *Physics Reports* **435**, 33 (2006).
- [32] P. Jacquod and C. Petitjean, Decoherence, entanglement and irreversibility in quantum dynamical systems with few degrees of freedom, *Adv. Phys.* **58**, 67 (2009).
- [33] G. Zhu, X. Lü *et al.*, Single-photon-triggered quantum chaos, *Phys. Rev. A* **100**, 023825 (2019).
- [34] B. Yan, L. Cincio, and W. H. Zurek, Information scrambling and loschmidt echo, *Phys. Rev. Lett.* **124**, 160603 (2020).
- [35] D. A. Roberts and D. Stanford, Diagnosing Chaos Using Four Point Functions in Two-Dimensional Conformal Field Theory, *Phys. Rev. Lett.* **115**, 131603 (2015).
- [36] J. Maldacena, S.H. Shenker and D. Stanford, A bound on chaos, *J. High Energ. Phys.* **08** (2016) 106.
- [37] K. Hashimoto, K. Murata and R. Yoshii, Out-of-time-order correlators in quantum mechanics, *J. High Energ. Phys.* **10** (2017) 138.
- [38] E. B. Rozenbaum, S. Ganeshan, and V. Galitski, Lyapunov Exponent and Out-of-Time-Ordered Correlator's Growth Rate in a Chaotic System, *Phys. Rev. Lett.* **118**, 086801 (2017).
- [39] I. García-Mata, M. Saraceno *et al.*, Chaos Signatures in the Short and Long Time Behavior of the Out-of-Time Ordered Correlator, *Phys. Rev. Lett.* **121**, 210601 (2018).
- [40] R. A. Jalabert, I. García-Mata, and D. A. Wisniacki, Semiclassical theory of out-of-time-order correlators for low-dimensional classically chaotic systems, *Phys. Rev. E* **98**, 062218 (2018).
- [41] C. Lin and O. I. Motrunich, Out-of-time-ordered correlators in a quantum Ising chain, *Phys. Rev. B* **97**, 144304 (2018).
- [42] H. Yan, J. Z. Wang, and W. G. Wang, Similar early growth of out-of-time-ordered correlators in quantum chaotic and integrable Ising chains, *Commun. Theor. Phys.* **71**, 1359 (2019).
- [43] M. McGinley, A. Nunnenkamp, and J. Knolle, Slow Growth of Out-of-Time-Order Correlators and Entanglement Entropy in Integrable Disordered Systems, *Phys. Rev. Lett.* **122**, 020603 (2019).
- [44] W. Zhao, Yue Hu *et al.*, Super-exponential growth of out-of-time-ordered correlators, *Phys. Rev. B* **103**, 184311 (2021).
- [45] M. Zonnios, J. Levensen, M. M. Parish, F. A. Pollock, and Kavan Modi, Signatures of Quantum Chaos in an Out-of-Time-Order Tensor, *Phys. Rev. Lett.* **128**, 150601 (2022).
- [46] D. A. Trunin, Refined quantum Lyapunov exponents from replica out-of-time-order correlators, *Phys. Rev. D* **108**, 105023 (2023).
- [47] S. Ruidas and S. Banerjee, Semiclassical Limit of a Measurement-Induced Transition in Many-Body Chaos in Integrable and Nonintegrable Oscillator Chains, *Phys. Rev. Lett.* **132**, 030402 (2024).
- [48] M. A. M. Aguiar and K. Furuya, Chaos in a Spin-Boson System: Classical Analysis, *Annals of Physics* **216**, 291-312 (1992).
- [49] L. Bakemeier, A. Alvermann, and H. Fehske, Dynamics of the Dicke model close to the classical limit, *Phys. Rev. A* **88**, 043835 (2013).
- [50] J. Chávez-Carlos *et al.*, Classical chaos in atom-field systems, *Phys. Rev. E* **94** 022209 (2016).
- [51] J. Chávez-Carlos *et al.*, Quantum and Classical Lyapunov Exponents in Atom-Field Interaction Systems, *Phys. Rev. Lett.* **122**, 024101 (2019).
- [52] S. Pilatowsky-Cameo *et al.*, Positive quantum Lyapunov exponents in experimental systems with a regular classical limit, *Phys. Rev. E* **101** 010202 (2020).
- [53] David Villaseñor *et al.*, Chaos and Thermalization in the Spin-Boson Dicke Model, *Entropy* **25**, 8 (2022).
- [54] D. Villaseñor *et al.*, Classical and Quantum Properties of the Spin-Boson Dicke Model: Chaos, Localization, and Scarring, arXiv:2405.20381.
- [55] M. A. B. Magnani *et al.*, Quantum multifractality as a probe of phase space in the Dicke model, *Phys. Rev. E* **109**, 034202 (2024).
- [56] J. Li and S. Chesi, Routes to chaos in the balanced two-photon Dicke model with qubit dissipation, *Phys. Rev. A* **109**, 053702 (2024).

- [57] I. I. Rabi, Space Quantization in a Gyating Magnetic Field, *Phys. Rev.* **51**, 652 (1937).
- [58] Q. Xie, H. Zhong, M. T. Batchelor, and C. Lee, *J. Phys. A: Math. Theor.* **50**, 113001 (2017).
- [59] J. Larson and T. Mavrogordatos, *The Jaynes-Cummings Model and Its Descendants* (IOP ebooks, 2021).
- [60] J. H. Eberly, N. B. Narozhny, and J. J. Sanchez-Mondragon, Periodic Spontaneous Collapse and Revival in a Simple Quantum Model, *Phys. Rev. Lett.* **44**, 1323 (1980).
- [61] E. K. T. Irish and A. D. Armour, Defining the Semiclassical Limit of the Quantum Rabi Hamiltonian, *Phys. Rev. Lett.* **129**, 183603 (2022).
- [62] A. V. Kirkova, D. Porras, and P. A. Ivanov, Out-of-time-order correlator in the quantum Rabi model, *Phys. Rev. A* **105**, 032444 (2022).
- [63] S. Wang, S. Chen, J. Jing, J. Wang, and H. Fan Quantum collapse and exponential growth of out-of-time-ordered correlator in anisotropic quantum Rabi model, arXiv:2305.17495
- [64] K. E. Cahill and R. J. Glauber, Density Operators and Quasiprobability Distributions, *Phys. Rev.* **177**, 1882 (1969).
- [65] J. Eiselt and H. Risken, Quasiprobability distributions for the Jaynes-Cummings model with cavity damping, *Phys. Rev. A* **43**, 346 (1991).
- [66] C. A. Miller, J. Hilsenbeck, and H. Risken, Asymptotic approximations for the Q function in the Jaynes-Cummings model, *Phys. Rev. A* **46**, 4323 (1992).
- [67] A. Alvermann, L. Bakemeier, and H. Fehske, Collapse-revival dynamics and atom-field entanglement in the nonresonant Dicke model, *Phys. Rev. A* **85**, 043803 (2012).
- [68] M. Ueda, T. Wakabayashi, and M. Kuwata-Gonokami, Synchronous Collapses and Revivals of Atomic Dipole Fluctuations and Photon Fano Factor beyond the Standard Quantum Limit, *Phys. Rev. Lett.* **76**, 2045 (1996).
- [69] G. Rempe, H. Walther, and N. Klein, Observation of quantum collapse and revival in a one-atom maser, *Phys. Rev. Lett.* **58**, 353 (1987).
- [70] A. Auffeves *et al.*, Entanglement of a Mesoscopic Field with an Atom Induced by Photon Graininess in a Cavity, *Phys. Rev. Lett.* **91**, 230405 (2003).
- [71] D. Lv, S. An, M. Um, J. Zhang, J. Zhang, M. S. Kim, and K. Kim, Reconstruction of the Jaynes-Cummings field state of ionic motion in a harmonic trap, *Phys. Rev. A* **95**, 043813 (2017).
- [72] G. Kirchmair *et al.*, Observation of quantum state collapse and revival due to the single-photon Kerr effect, *Nature (London)* **495**, 205 (2013).